TELKOMNIKA Telecommunication, Computing, Electronics and Control
Vol. 18, No. 1, February 2020, pp. 465~475
ISSN: 1693-6930, accredited First Grade by Kemenristekdikti, Decree No: 21/E/KPT/2018
DOI: 10.12928/TELKOMNIKA.v18i1.12447

A novel cross-coupled microstrip bandpass filter with hairpin-DGS resonators using coupling matrix technique

Chetioui Mohammed[1], Bouasria Fatima[2], Damou Mehdi[3]
[1]Laboratory of Telecommunications, University of Aboubekr Belkaid of Tlemcen, Algeria
[2]Laboratory of Knowledge Management and Complex Data, University of Dr. Moulay Tahar of Saïda, Algeria
[3]Laboratory of Technologies of Communications, University of Dr. Moulay Tahar of Saïda, Algeria

Article Info

Article history:

Received Jan 28, 2019
Revised Oct 7, 2019
Accepted Oct 27, 2019

Keywords:

Coupling matrix (CM)
Cross coupling (CC)
Hairpin-defected ground structure (Hairpin-DGS)
Microstrip bandpass filter (MBPF)
Transmission zeros

ABSTRACT

This paper introduces a new design of a cross-coupled microstrip bandpass filter (MBPF) based on hairpin defected ground structure (DGS) resonators using accurate coupling matrix (CM) technique for microwave communication systems. The article presents the equivalent circuit of the suggested MBPF based on the DGS equivalent circuit model derived from the equivalent inductance and capacitance that occurs despite the presence of the slots disrupting the current in the ground layer. The paper investigates also the different external coupling mechanisms that the feed configuration affects significantly the filter response. In this paper, a four order Chebyshev topology has been adopted for designing the filter to suppress harmonics and achieve a very compact size and a wide stopband with two transmission zeros.

Corresponding Author:

Chetioui Mohammed,
Laboratory of Telecommunications,
University of Aboubekr Belkaid of Tlemcen, Algeria.
Email: chetioui.mohammed@yahoo.fr

1. INTRODUCTION

High performance and lightweight filtering mechanisms often only satisfy the rigorous demands of modern microwave communication systems. The coupled microstrip bandpass filter has been widely realized and broadly used in several microwave systems to obtain high performance, small area and low charge and to meet strictly necessary transmission requirements. Several of these filters were documented using framework called the defected ground structures that are investigated by etching off a defective ground layer pattern [1]. An etched defect disrupt the distribution of the shield current in the ground layer [2]. Seeing as DGS cells have necessarily resonant properties, they were used to enhance the stop and pass-band characteristics in the filtering circuits. The DGS was suggested to improve the suppression of fictitious response of low-pass filters from microstrips and coupled band-pass filters from microstrip line. DGS is not seen as the central building blocks in all these reports; rather, they are used to impro ve the response of the already built instruments such as couplers and filters [3, 4]. The fast growth of modern wireless communication has increased the demand for compact, low cost and high-performance components. One of the essential components of modern wireless communication systems is the microstrip filter [5-7]. Microstrip low-pass filter of extremely-wide stopband is also a very important part in wireless transmission structures for the suppression of undesired higher frequency harmonics. The modern wireless communication demands compact filters with with low insertion loss and elevated passband return loss and large stopband disallowance.

In this context, this paper presents a design of a cross-coupling microstrip bandpass filter focused on hairpin-defected ground structure resonators using accurate matrix technique for microwave communication systems [8-10]. The com parable circuit of the suggested section of the DGS unit is derived use the field analysis technique [11, 12]. The results of the simulation create good consistency with the theoretical findings with a broad suppression of harmonics, a very compact size and a small stop band with two transmission zeros.

2. MEMS HAIRPIN-DGS CELL FREQUENCY CHARACTERISTICS

The Figure 1(a) demonstrates a DGS cell in the shape of a hairpin with a microstrip line 50-Ohm on top. The DGS is carved in the ground layer of bottom metal [13, 14]. The EM simulation is carried in for a substrate at a relative dielectric of ε_r = 3.38 and a thickness of h = 0.813 mm. The fifty-Ohm microstrip section is w = 1.85 mm in width and the hairpin-DGS dimensions are: a = 15.5 mm, b = 12.5 mm, c = 4.5 mm, f = 3 mm, g = 0.5 mm, w_r = 1.5 mm as exposed in Figure 1 (b). DGS cells are analyzed using High Frequency Structure Simulation (ANSYS-HFSS) software [15, 16]. Figure 1 (c) indicates the characteristic of a one-pole low-pass filter with an attenuation pole frequency f_0 at 5.2 GHz and a cutoff frequency of -3 dB f_c as shown in Table 1.

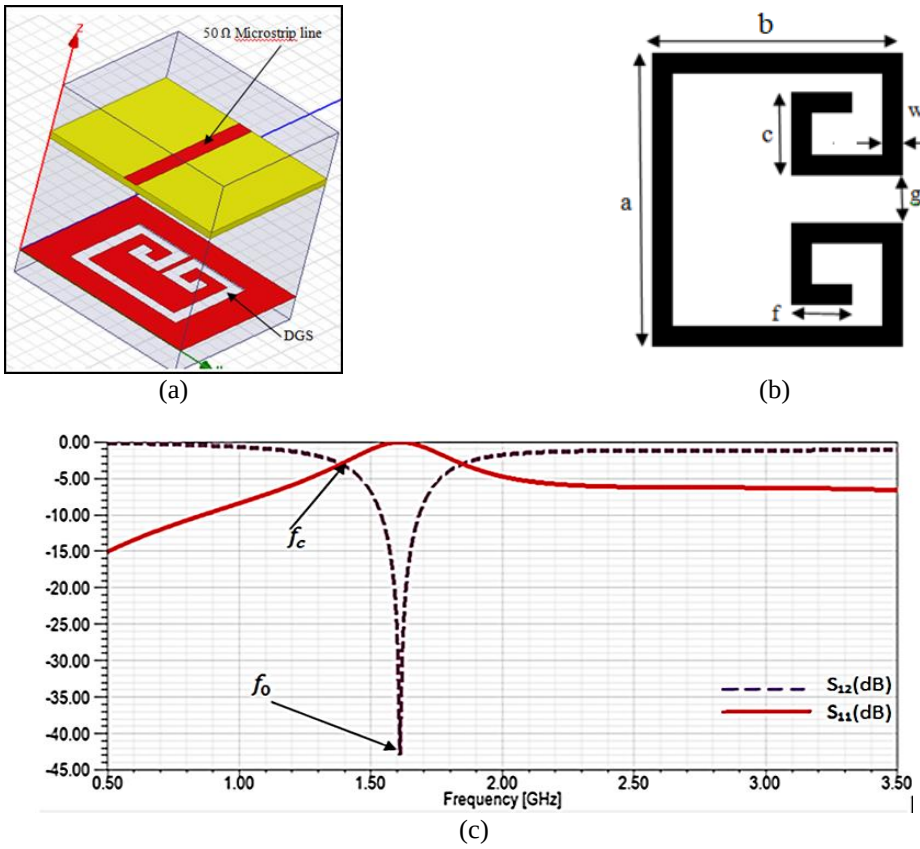

Figure 1. Proposed Hairpin-DGS cell: (a) 3D view, (b) dimenssions, (c) simulated S-parameters

3. FIELD ALLOCATION OVER THE CELL HAIRPIN-DGS

This section aims at investigating the reliance of the corresponding circuit elements (inductance and capacity) on the substrate known as propagation of electromagnetic fields. The electric field is heavily concentrated in the gap in Figure 2 (a), so any change in the parameters of the gap influences the structure's effective capacitance [17, 18]. The calculated magnetic and electrical field densities using HFSS are seen in Figure 2 (b). Which can be seen, the magnetic field is focused across the central ground line, so the central ground line determines the inductance. The electric field is distributed across the engraved spaces, reflecting the capacitance [17-19]. The slot-head region regulates essentially the inductance [20, 21] while the linking shaped slot width "g" regulates the capacitance [22, 23].

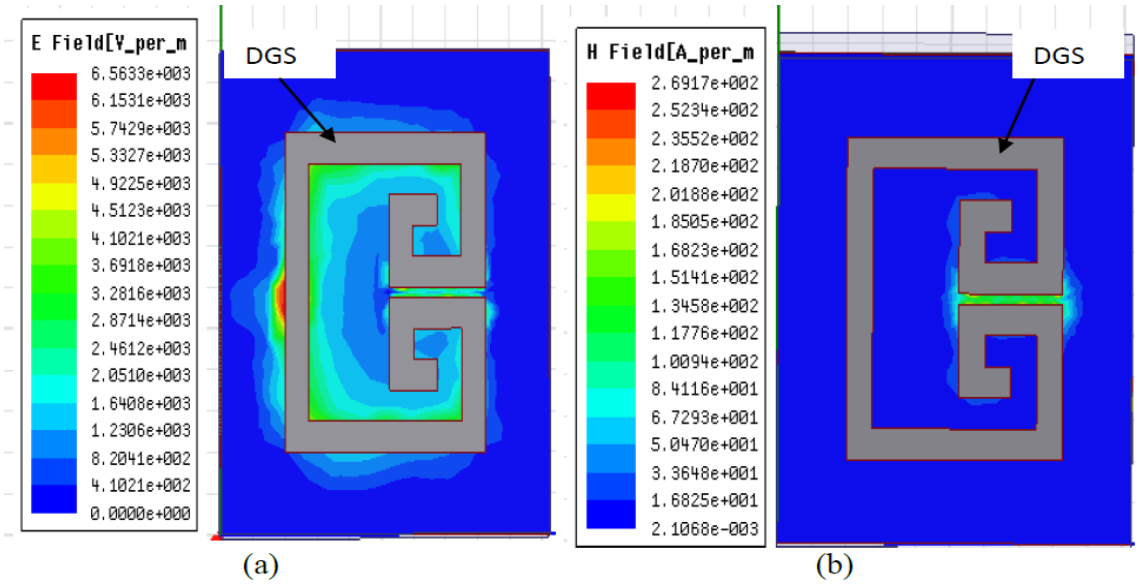

Figure 2. Electromagnetic field perturbation over the Hairpin-DGS cell:
(a) electric field density, (b) magnetic field density

4. MODELING PARAMETER EXTRACTED OF HAIRPIN-DGS CELL

A simplified equivalent circuit model for the hairpin-slot of DGS structure for the suggested filter is presented in Figure 3. The LP and CP parameters can be derived from the hairpin-DGS cell's transmission characteristics using traditional techniques [24]:

$$C_p = \frac{5 f_c}{\pi\left(f_o^2 - f_c^2\right)} \quad pF \tag{1}$$

$$L_p = \frac{250}{C_p\left(\pi f_o\right)^2} \quad nH \tag{2}$$

from Figure 1 (b), f_c with GHz is the cut-off frequency of the stopband response of the slot at -3 dB and f_0 with GHz is its zero transmision. Efficiency C_{gap} refers to the coupling between the central ground line and the metallization of the internal metal arms contribution [25], whereas C_2 contributes to the internal metal arms efficiency contribution. C1 refers to the contribution made by the hairpin-DGS cell to ability without any of the influence of the internal metal arms. C_1, C_2 and C_{gap} can be determined from three distinct model transmission properties of three hairpin-DGS cell variations. The open loop square filters variations are shown in Figures 4, 5 and 6.

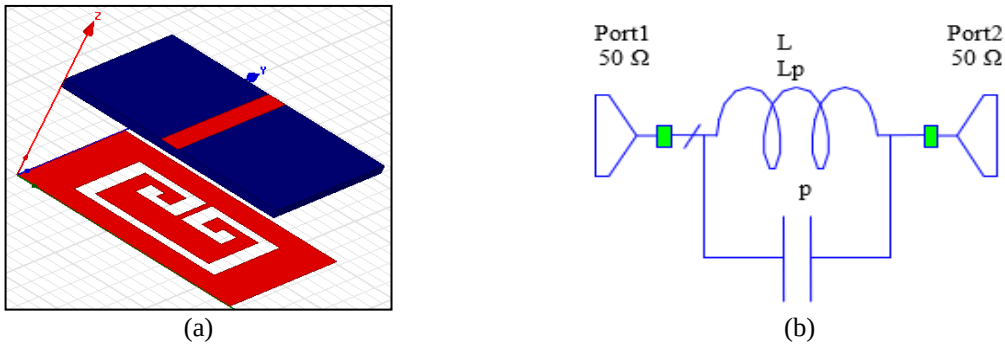

Figure 3. Hairpin-DGS cell: (a) HFSS elements, (b) extracted equivalent circuit elements

4.1. First variation

Without the inner metal, so $C_2 = 0$ and $C_{gap} = 0$ resulting in:

$$C_1 = C_{v1} = 1.4719 \text{ pF} \quad (3)$$

where C_{v1} for the first variation is the standard circuit parameter from (1).

4.2. Second variation

Without the difference between the center ground transmission line and the internal metal arms (respectively $C_{gap} = \infty$) leading in:

$$C_2 = C_1 - C_{v2} \quad (4)$$

when C_{v12} for the second variation is the standard circuit parameter (1), C2 = 4,338 pF.

4.3. Third variation

To the gap between the center ground transmission line and the internal metal arms leading in:

$$C_{gap} = \frac{C_2}{\left(\frac{C_2}{(C_{v3}-C_1)}-1\right)} \quad (5)$$

where C_{v3} is the standard circuit parameter for 3rd variation from (1), C_{gap} = 3.318 pF. The equivalent circuit parameters for C_1 = 1.4719 pF, C_2 = 4.338 pF, C_{gap} = 3.3182 pF, L_p = 2.845 nH are extracted as shown the Table 1. The thorough equivalent hairpin-DGS cell circuit can be seen in Figure 7.

Table 1. Data derived and measured for the three Hairpin-DGS cell variations

	1st variation	2nd variation	3rd variation
f_c in GHz	1.9	1.2	1.39
f_0 in GHz	2.38	1.33	1.61
C in pF	C_{v1}= 1.4719	C_{v2} = 5.81	C_{v3} = 3.352

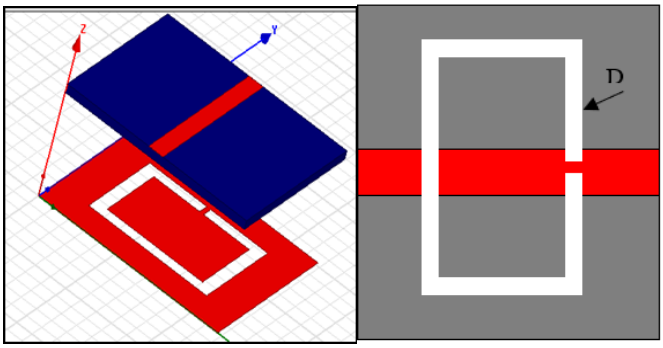

(a)

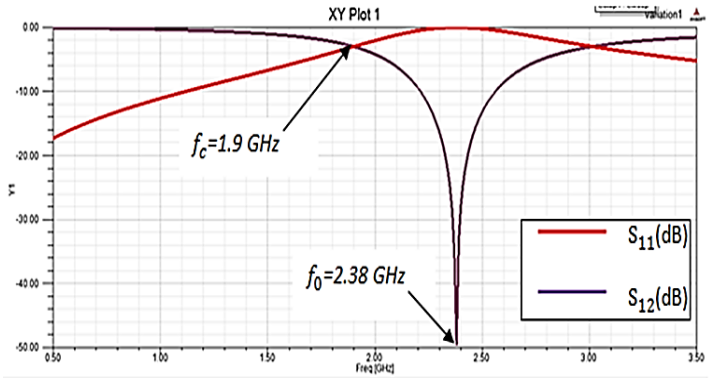

(b)

Figure 4. Hairpin-DGS cell 1st variation:
(a) topology of the conceptual hairpin cell-DGS, (b) results S-parameters

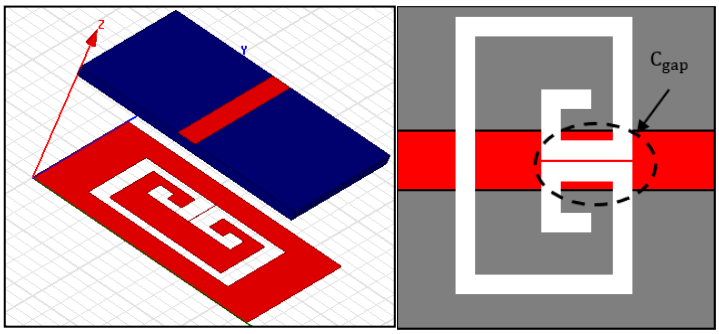

(a)

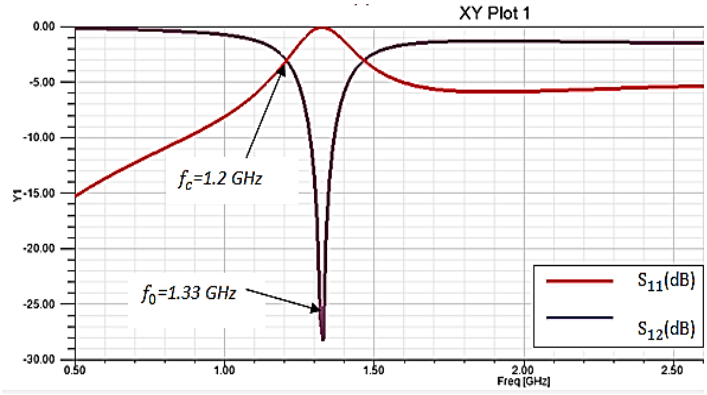

(b)

Figure 5. Hairpin-DGS cell 2nd Variation:
(a) topology of the conceptual hairpin cell-DGS, (b) results S-parameters

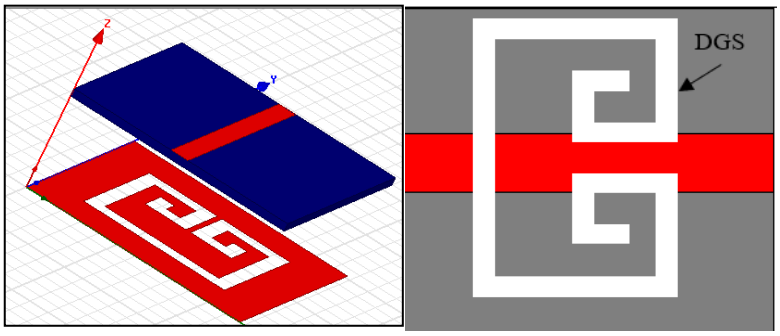

(a)

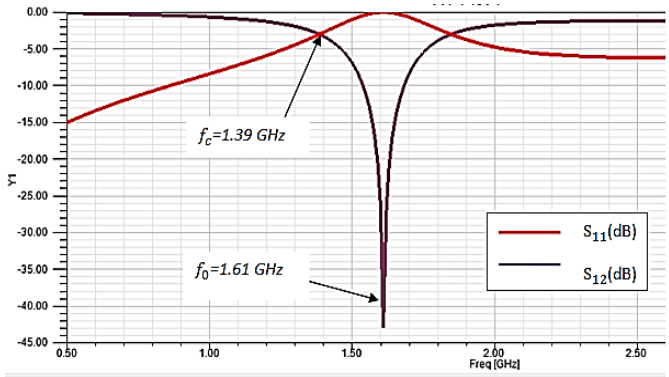

(b)

Figure 6. Hairpin-DGS cell 3rd Variation:
(a) topology of the conceptual hairpin cell-DGS, (b) results S-parameters

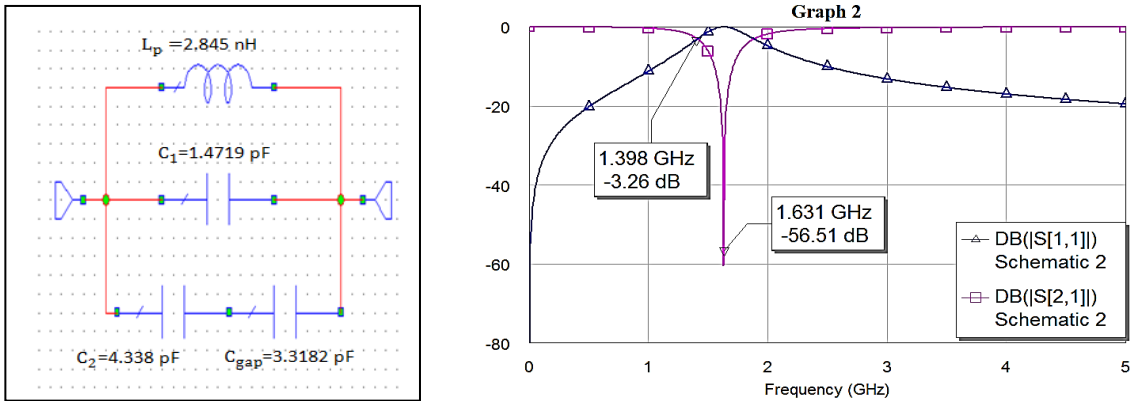

(a) (b)

Figure 7. Hairpin-DGS cell: (a) equivalent circuit, (b) simulated S-parameters

5. DESIGN OF THE SECOND ORDER MBPF USING HAIRPIN-DGS CELL

In order to achieve a useful design microstrip bandpass filter, two of the hairpin-DGS cells (resonators) already identified were combined. The MBPF is simulated with a center frequency f_0= 1.34 GHz and a fractional bandwidth FBW = 11.8% with return loss RL = 20 dB. Both resonators are symmetric and isolated by a distance S as seen in Figure 8. Two fifty-Ohm microstrip lines symmetrically feed the DGS hairpin resonators. The nature of the feed used influences the filter response.

A symmetrical Chebyshev response is obtained by using the feed arrangement seen in Figure 9. The external quality factor is obtained by changing the expanded stub. The resonant frequency of the cavity is sensible to the length of the stub. Figure 10 shows the response of the one transmission zero because the feeding lines pass very close to the second resonator and are poorly coupled. The transmission zero location can be operated by increasing the feed lines to fifty-Ohm. Two transmission zeros are obtained as shown in Figure 11, due to the cross-coupling between the input and the output ports. By changing the distance between the fifty microstrip feed lines, the location of the transmission zeros can be controlled.

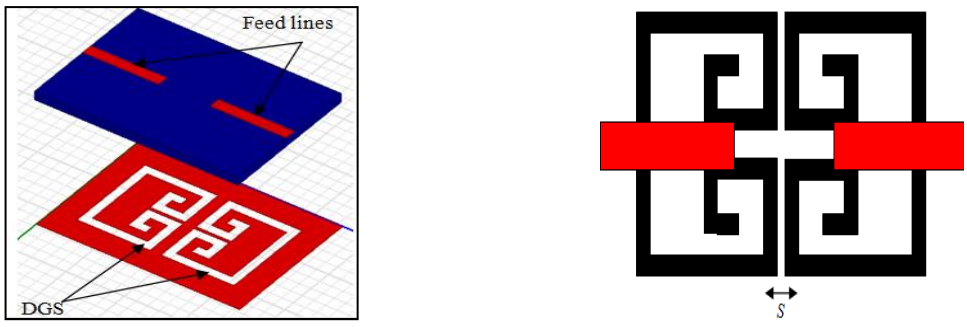

(a) (b)

Figure 8. Coupled hairpin-DGS MBPF: (a) 3D view, (b) layout

6. DESIGN AND SIMULATION OF THE NOVEL HAIRPIN-DGS MBPF

6.1. External quality factor and coupling parameters

Figure 12 illustrates the various coupling configurations that are appropriate for the design of MBPF cross-coupling resonator. The shapes a, b and c are the result of various orientations of a couple of hairpin-DGS resonators isolated by distance S using a substrate with a relative dielectric ε_r = 3.38 and a thickness h = 0.813 mm. The coupling coefficients [4, 6] shown in the Figure 12 are determinated using the EM HFSS by coupling the configuration to a fifty-OhmΩ feed line. From distance frequencies the coupling coefficients can be calculated.

s shown in Figure 13, the external quality factor [4] is built at the other part of a substrate by a fifty-Ohm microstrip line with a relative dielectric ε_r =3.38, the external quality factor value is derived from the ANSYS HFSS simulator. These resonant frequencies do not significantly change whenever the feed line is slightly moved by a distance d.

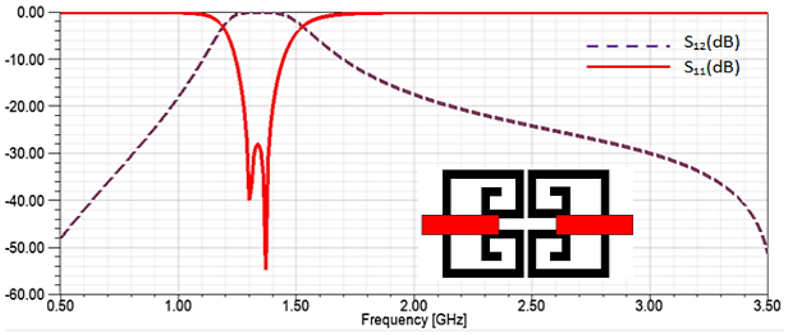

Figure 9. Compact second order coupled resonators MBP filter (with the first feeding configuration)

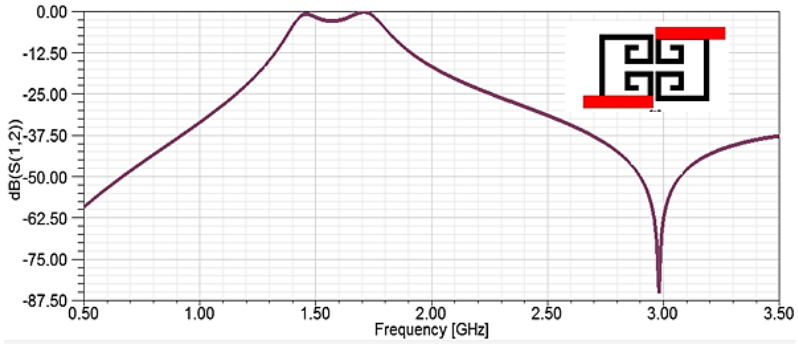

Figure 10. Compact second order coupled resonators MBP filter (with the second feeding configuration)

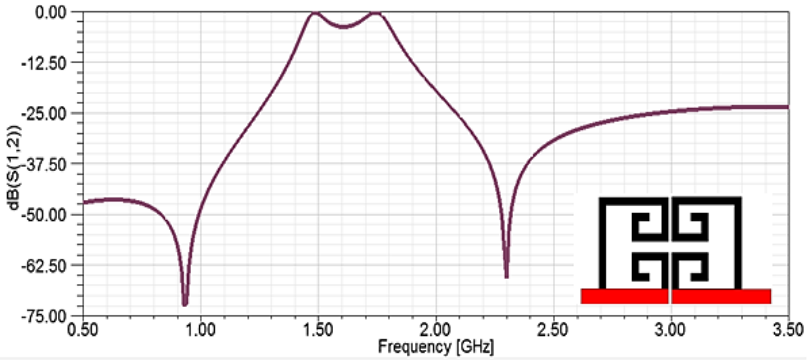

Figure 11. Compact second order coupled resonators MBP filter (with the third feeding configuration)

6.2. Simulation of the improved hairpin-DGS MBPF

A multilayer structure is used to increase the efficiency of the traditional band-pass filter. The novel scheme is similar to the current filter but, as shown in Figure 14, the cross-coupled resonators are shifted to the bottom layer as hairpin-DGS. This suggested geometrical concept is based on using many layered layers. This was observed to increase the efficiency and to reduce the overall filter size. The filter is simulated with f_0 = 1.2 GHz and FBW = 91.7 %. In this situation a four-order filter was guessed, the coupling matrix extracted for the coupling and the external quality factor from the optimization scheme [5] are as continues to follow:

$$m = \begin{bmatrix} 0 & -0.1577 & 0 & 0.0008 \\ -0.1577 & 0 & -0.1236 & -0.0198 \\ 0 & -0.1236 & 0 & 0.1564 \\ 0.0008 & -0.0198 & 0.1564 & 0 \end{bmatrix} \quad (6)$$

$$Q_{in} = Q_{out} = 5.9126$$

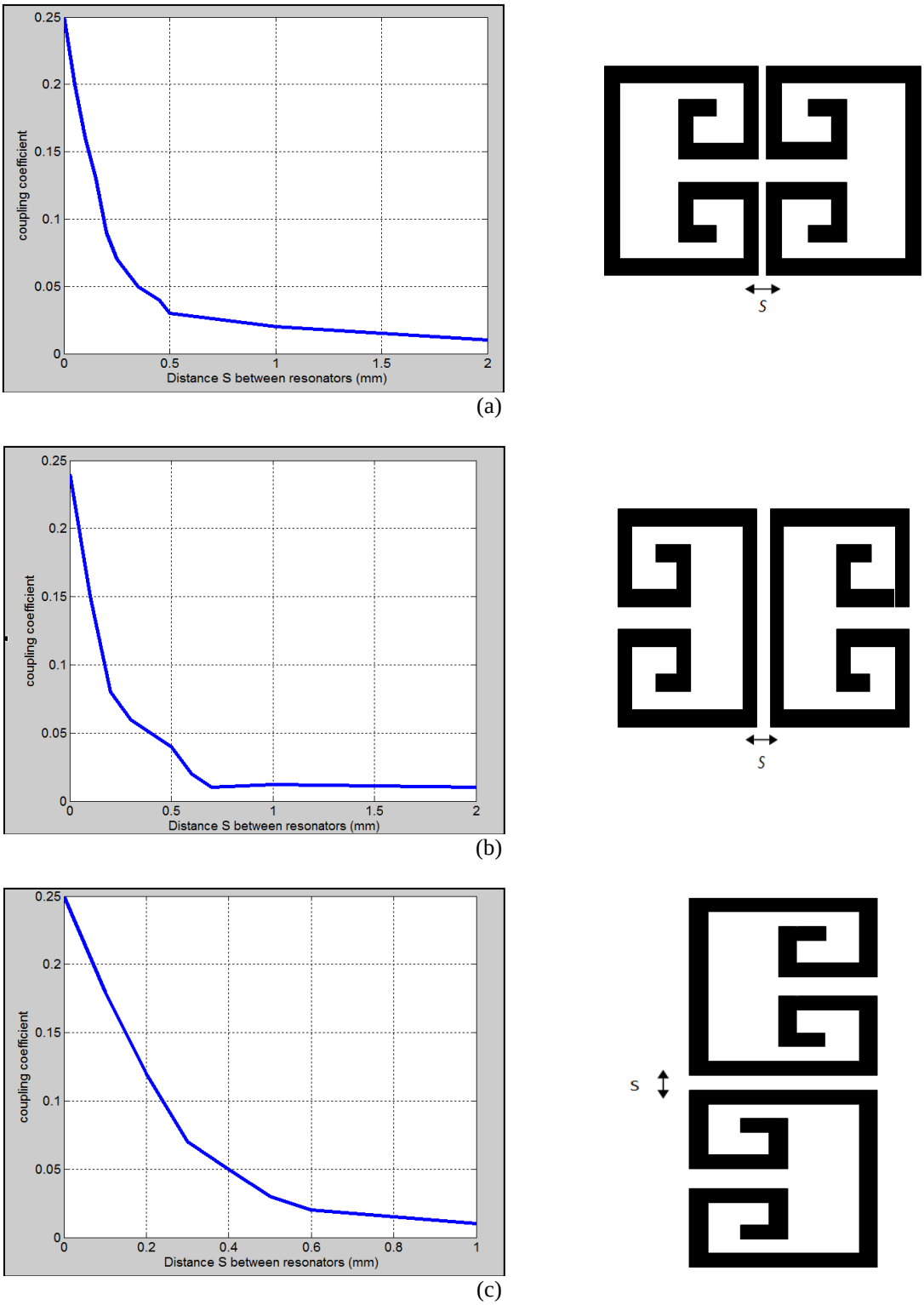

Figure 12. Coupling coefficients for the different hairpin-DGS clees: (a) magnetic Attraction, (b) electric attraction and (c) mixed attraction

The suggested hairpin-DGS MBPF was designed to simulate on even a substrate (relative dielectric ε_r of 3.38 and a thickness h of 0.813 mm). The EM simulation results of the cascaded MBPF and the compact multilayer bandpass performed using HFSS are shown in Figure 15. The simulated quality of the suggested four order MBPF is presented in Figure 15 (b). The EM simulated results indicate a center

frequency of 1.2 GHz, a FBW of 91.7%, a typical insertion loss of 1.05 dB and a typical return loss of 13.8 dB. That can be seen from Figure 15 (b) that the simulated results indicate best uniformity with simulation results Figure 15 (a). The simulated compact multilayer MBPF with hairpin-DGS has a middle frequency of 1.2 GHz and a suppression grade of 20 dB between 1.9 and 3.5 GHz; the passband insertion los s is around 1.05 dB. This demonstrates that the suggested compact multilayer coupled hairpin-DGS MBPF has significantly enhanced efficiency as opposed to the cascaded MBPF without the hairpin-DGS.

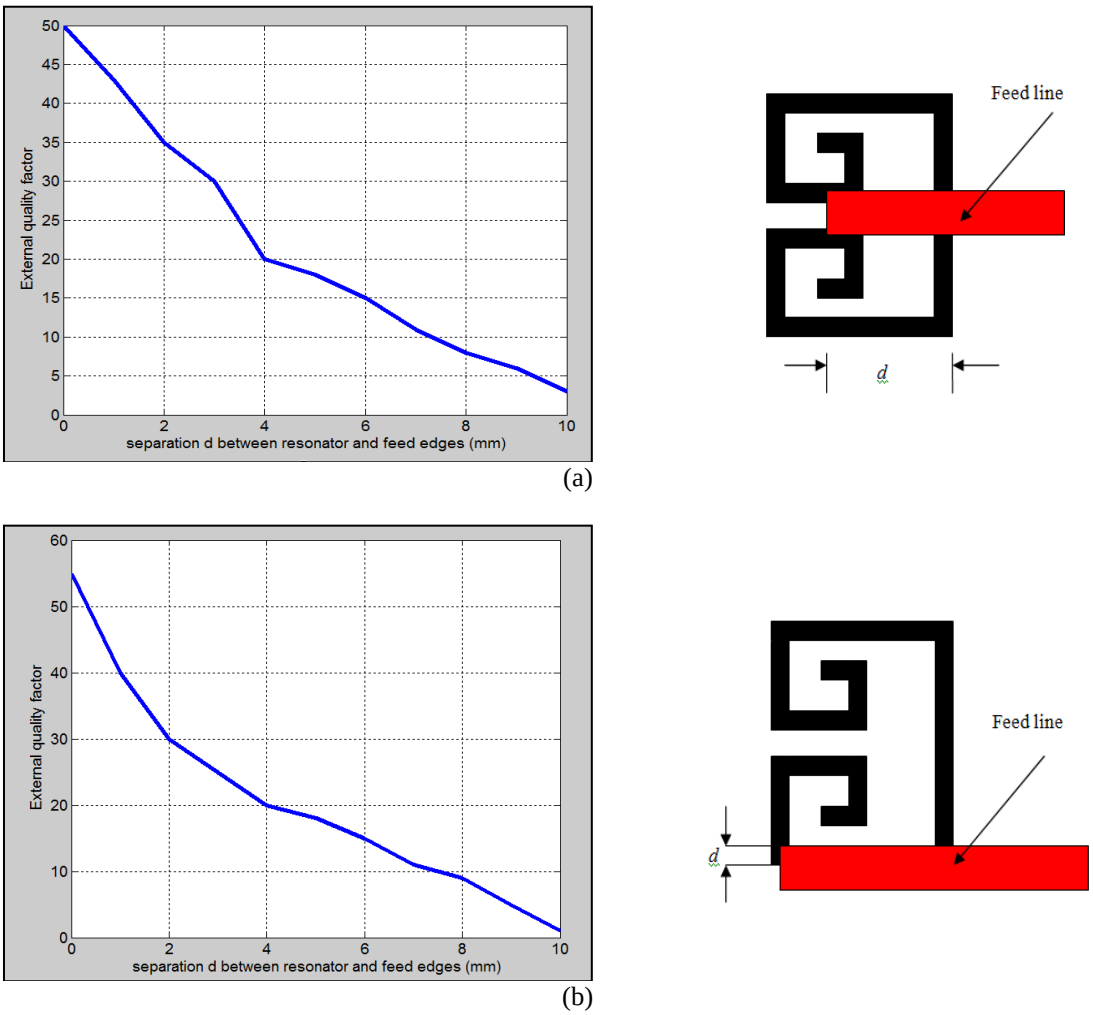

Figure 13. External quality factor changes: (a) 1st feeding position, (b) 2nd feeding position

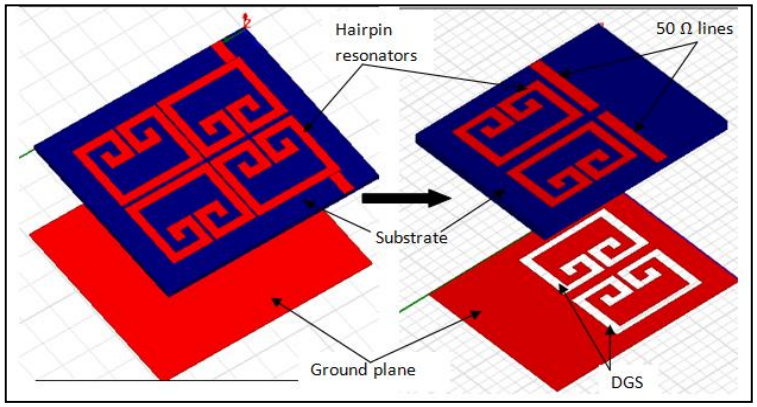

Figure 14. 3D visualization of the cascaded MBP filter transition (left) to compact multilayer MBP filter (right)

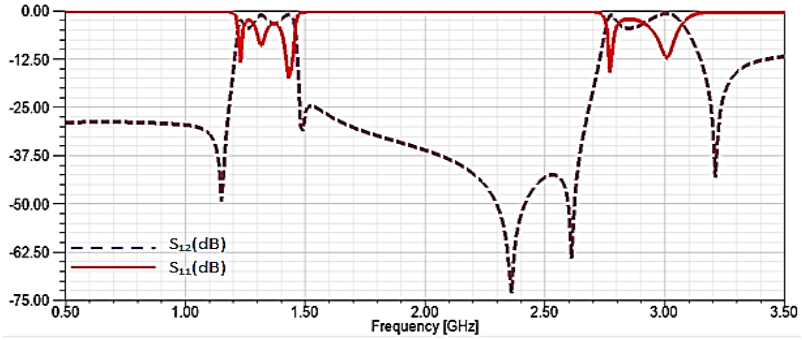

(a)

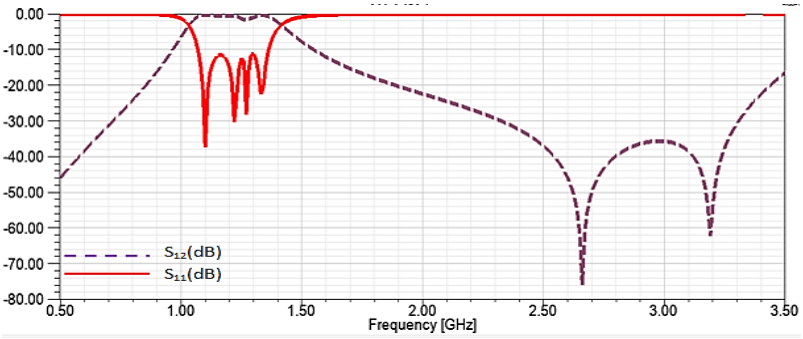

(b)

Figure 15. Simulation results: (a) of the cascaded MBP filter without hairpin-DGS, (b) to compact multilayer MBP filter with hairpin-DGS

7. CONCLUSION

In this work a new design of a cross-coupled microstrip bandpass filter based on hairpin defected ground structure resonators using accurate coupling matrix technique has been proposed for microwave communication systems. The paper describes the filter equivalent circuit model and investigates the influence of its geometrical parameters on its resonance and cutoff frequencies. The paper demonstrates that the feeding configuration affects significantly the filter response after having investigated its different external coupling mechanisms. A new four order MBP filter using coupling matrix extraction with a middle frequency of 1.2 GHz and a FBW of 91.7% has been achieved by moving the cross coupled resonators to the bottom ilter layer forming hairpin-DGS resonators to improve the efficiency of the MBP filter and Removes the harmonics.

REFERENCES

[1] A. R. Ali, et al., "Direct Cross-coupled Resonator Filters Using Defected Ground Structure (DGS) Resonators," *IEEE Microwave and Communication Engineering, microwave conference*, 2005.
[2] M. Awida, et al., "Multi-bandpass Filters using multi-armed split ring resontors with direct feed," *IEEE M/T-S International Microwave Symposium, Honolulu, Hawaii*, pp. 913-916, Jun 2007.
[3] J. K. Xiao, et al., "Novel compact split ring stepped-impedance resonator (sir) bandpass filters with transmission zeros," *J. Electromagn. Waves Appl*., vol. 21, no. 3, pp. 329-339, 2007.
[4] J. S. Hong and M. J. Lancaster, "Microstrip Filters for RFIMicrowave Applications," Wiley, New York, 2001.
[5] R. J. Cameron, et al., "Microwave Filters for Communication Systems: Fundamentals, Design, and Applications," Wiley, 2007.
[6] S. Jovanović and A. Nešić, "Microstrip bandpass filter with new type of capacitive coupled resonators," *Electronics Letters*, vol. 41, no. 1, pp. 19-21, Jan 2005.
[7] L. Singh and P. K. Singhal, "Design and Analysis of Hairpin Line Bandpass Filter," *International Journal of Advanced Research in Electronics and Communication Engineering (IJARECE)*, vol. 2, no. 2, pp. 228-230, Feb 2013.
[8] L. Fei, et al., "Novel Compacttriple-bandpass filter using λ/4 resonator pairs with common via ground," *Proceeding of the Progress in Electromagnetics Research Symposium*, pp. 1220-24, 2012.

[9] S. Amari and M. Bekheit, "Physical interpretation and implication of similarity transformation in coupled resonator filter design," *IEEE Trans. Microw. Theory Tech.*, vol. 55, no. 6, pp. 1139-1153, Jun 2007.
[10] E. Shih and J. T. Kuo, "A new compact microstrip stacked-SIR bandpass filters with transmission zeros," in *2003 IEEE MTT-S Int. Microwave Symp. Dig., Philadelphia, Pennsylvania*, pp. 1077-1080, Jun 2003.
[11] L. Szydlowski, et al., "Coupled-resonator filters with frequency-dependent couplings: Coupling matrix synthesis," *IEEE Microw. Wireless Compon. Lett.*, vol. 22, no. 6, pp. 312-314, Jun 2012.
[12] J. S. Lim, et al., "A new type of low pass filter with defected ground structure," *European Microwave Week, Milan, Italy*, Sep 2002.
[13] D. Ahn, et al., "A Design of the Lowpass Filter Using the Novel Microstrip Defected Ground Structure," *IEEE Trans. MTTs*, vol. 49, no. 1, pp. 86-93, Jan 2001.
[14] A. Boutejdar, et al., "A Compact Microstrip Multi-Layer Lowpass Filter Using Triangle Slots Etched in the Ground Plane," *Proc. 36th European Microwave Conference 2006 (EuMC), Manchester, UK*, Sep 2006.
[15] A. Boutejdar, et al., "A Novel Method to Obtain a Large Reject- Band with a Compact Bandstop Filter Using Dected Ground Structure (DGS) Coupled Resonators," *MMS 2006 Mediterranean Microwave Symposium, Genova, Italy*, 2006.
[16] A. S. S. Mohra, "Compact lowpass filter with sharp transition band based on defected ground structures," *Progress in Electromagnetics Research Letters*, vol. 8, pp. 83-92, 2009.
[17] A. Boutejdar, et al., "Design of a novel ultrawide stopband lowpass filter using a DMS-DGS technique for radar applications," *International Journal of Microwave Science and Technology*, vol. 2015, pp. 1-7, 2015.
[18] A. Boutejdar, "Design of compact reconfigurable broadband band-stop filter based on a low-pass filter using half circle DGS resonator and multi-layer technique," *Progress In Electromagnetics Research C*, vol. 71, pp. 91-100, 2017.
[19] A. Boutejdar, et al., "LPF builds on Quasi-Yagi DGS," *Microwaves & RF*, vol. 52, pp. 72-77, 2013.
[20] A. Balalem, et al., "Quasi-elliptic microstrip low-pass filters using an interdigital DGS slot," *IEEE Microw. Wireless Compon. Lett.*, vol. 17, no. 8, pp. 586-588, Aug 2007.
[21] P. M. Raphika, et al., "Compact low pass filter with a sharp roll-off using patch resonators," *Microwave and Optical Technology Letters*, vol. 56, vol. 11, pp. 2534-2536, 2014.
[22] X. Chen, et al., "Compact lowpass filter with wide stop band bandwidth," *Microwave and Optical Technology Letters*, vol. 57, no. 2, pp. 367-371, 2015.
[23] L. Wang, et al., "Design of compact microstrip low-pass filter with ultra-wide stopband using SIRs," *Progress in Electromagnetics Research Letters*, vol. 18, pp. 179-186, 2010.
[24] H. Cao, et al., "Compact lowpass filter with high selectivity using G-shaped defected microstrip structure," *Progress in Electromagnetics Research Letters*, vol. 33, pp. 55-62, 2012.
[25] A. Auob and L. Ali, "Compact lowpass filter with wide stop-band using open stubs loaded spiral microstrip resonant cell," *Applied Computational Electromagnetics Society Journal*, vol. 28, no. 1, pp. 27-34, Jan 2013.